ISSN-1996-918X

Pak. J. Anal. Environ. Chem. Vol. 18, No. 1 (2017) 69 – 83

http://doi.org/10.21743/pjaec/2017.06.07

Adsorption of 4-Nitrophenol Using Pilli Nut Shell Active Carbon

F. O. Nwosu*, F. A. Adekola and A. O. Salami

Department of Industrial Chemistry, Faculty of Physical Sciences, University of Ilorin, Ilorin, Nigeria

*Corresponding Author Email: f.o.nwosu@gmail.com

Received 30 March 2016, Revised 09 June 2017, Accepted 23 June 2017

Abstract

An economically feasible technology for the removal of pollutants from wastewater is adsorption. Active carbon was prepared by single stage method via chemical impregnation of pili Nut-Shell (PNS) with orthophosphoric acid and activation at a temperature of 450^{o}C using precursor-acid ratio of 1:4 for a period of 2 h. The effects of initial concentration, contact time, adsorbent dose and pH on the uptake of 4-nitrophenol / para-nitrophenol (PNP) using pili nut-based active carbon (PAC) were determined. The PAC maximum adsorption capacity value (190.39 mg/g) was obtained at an initial concentration of 1000 mg/L and was found to be greater than that of a commercial granular active carbon (CGAC) (166.97 mg/g) at an initial concentration of 800 mg/L. The BET surface area and total pore volume of PAC (960 m^2/g, 0.422 cm^3/g) respectively were also greater than that of CGAC (426.3 m^2/g, 0.208 cm^3/g). The pore size distribution of the PAC (2.842 nm) classifies it to be within range of super-microporous and as such could be used for toxic gas removal as well as small liquid molecules. The Langmuir isotherm best described the adsorption of PNP onto PAC, while pseudo second order kinetics fitted best. The adsorption process was exothermic and spontaneous. Thus, active carbon produced from PNS can be used to adsorb PNP.

Keywords: Pili nut, 4-Nitrophenol, Active carbon, Kinetics, Isotherm, Thermodynamics

Introduction

Aquatic organisms and human are normally endangered because of frequent discharge of wastewater into surface water bodies. The major sources of phenols in surface and underground water are industrial effluents, domestic wastewaters, agricultural effluents and spillage of chemicals from anthropogenic activities [1]. The continuous exposure to low levels of phenol in water may cause diarrhoea, mouth ulcers, anaemia, dark urine, and damage of liver. Humans and other living organisms could suffer mutagenesis and carcinogenesis as a result of phenol contamination [2]. It has been asserted that death of animal may result if dilute phenol solution is spilled to cover area greater than 25% of its total body surface [3]. The Bureau of Indian Standards (BIS) [4] permissible limit of phenol as 1.0 g/L for drinking water.

The phenolic pollutants in most effluents could be treated using microbial organisms, chemical oxidation as well as photocatalytic degradation with aid of TiO_2 [5]. Enzymatic polymerization and adsorption principles have been found useful for remediation of phenol polluted wastewater [6]. Among others, selective adsorptions that make use of biological materials and active carbon have created great interest among the researchers.

Organic pollutants are adsorbed onto active carbon due to its large surface area but active carbon is difficult to prepare and exhibits higher disposal cost [6]. The preparation and regeneration of active carbon made scientists to search for the development of adsorbents from cheaper raw materials. These include active

carbons prepared from tamarind nut [7] and coconut husk [8] for the removal of phenolic compounds. Therefore, the preparation of high grade active carbons via chemical activation of PNS (waste material) for removal of low concentration of phenol molecules becomes inevitable.

The main aim of this study was the preparation of low cost and environmentally safe active carbon adsorbent and its use for removal of 4-nitrophenol from wastewater compared with commercial active carbon adsorbent. Thus, the PNS, which are wastes, were converted into cheap carbonaceous adsorbents. Batch adsorption and kinetics studies were carried out and data modeled into various adsorption models.

Materials and Methods

Materials

The precursor, pili nut (*Cannarium Ovatum*) shell was utilized for the preparation of active carbon. The mature pili nuts were harvested from its plant in Anambra State, Nigeria located at Latitude and Longitude 6^o 1′ 0″ N, 6^o 55′ 0″E. It was then stripped by boiling to expose the nuts. The nuts were washed with distilled water to remove impurities, air dried and de-shelled. It was crushed with hammer mill into small sizes.

Preparation of active carbon

A known quantity (40.0 g) of PNS was impregnated with 4 M H_3PO_4 using acid to precursor ratio of 1:4; w/v. It was heated with a low heat and was placed in an oven maintained at 383 K for 7 h. The horizontal tubular furnace was first degassed by allowing N_2 to flow into the reactor at 1000 mL/min for 30 mins. The mixture was then carbonized in a horizontal tubular furnace under a flow of N_2 gas (500 mL/min) for 2 h. The carbonization procedure was carried out at 723 K. The activated sample was cooled to room temperature under N_2 flow, washed with de-ionized water several times until pH 6-7 was obtained. It was then filtered under vacuum and dried in oven at 383 K for 8 hours. The dried samples were grounded, sieved to < 150 µm and stored in airtight plastic containers [9].

Characterization of active carbon

The standard test method of ASTM D 3838-60 [10] was used to determine the pH of the active carbon. The same samples used for pH determination were used further for electrical conductivity of the active carbon and results were read off [11].

Moisture content of active carbon and raw materials were obtained by utilizing ASTM D 2867-9110 method [10] while their densities were obtained via tamping procedure [12].

Structural analysis of active carbon

The surface morphology of the active carbon was examined by Scanning Electron Microscope (SEM) using a Phenon World Scanning Electron Microscope. The crystalline nature of the active carbons was compared using a Shimadzu X-ray diffractometer, Model 6000 machine. A Perkin Elmer 1600 Series FTIR Spectrophotometer Model 1615 was used in the evaluation of functional groups present on the active carbon after crushing with nujol. The Brunauer −Emmett − Teller (BET) method was adopted for N_2 adsorption at 77K on to active carbons and data obtained were used for determination of surface area, pore volumes and pore size distribution of the active carbons. Prior to nitrogen adsorption measurement, active carbons were separately degassed at 323 K.

Factors affecting adsorption

Distilled water was used to prepare stock solution of the test reagents; 1 g of PNP was dissolved in 1 L of distilled water. Other concentrations were prepared by serial dilution using micro pipettes and standard volumetric flasks. In each of the factors studied, the PNP uptake, q_t was calculated using the following expression:

$$q_t = \frac{(C_o - C_f)v}{m} \quad (1)$$

where q_t is the quantity of PNP uptake in mg/g, v is volume (L), C_o and C_f are the initial and final concentrations in mg/L respectively. The plastic containers containing the mixture of various PNP

concentrations and active carbons were then separately removed from the isothermal shaker and the solutions centrifuged to remove the adsorbent. The residual aqueous concentrations of PNP were then determined using UV- visible CamSpec M106 Spectrophotometer. Prior to determination using UV- visible techniques, the effect of variables on adsorption capacities of PAC and CGAC were done as follows:

Effect of initial concentration: Adsorption was carried out in a set of plastic sample containers where 25 mL of PNP solutions of different initial concentrations ranging from 100 mg/L to 1400 mg/L were placed. Equal amount of activated carbon (0.03 g) was added to each set of solution and kept on an isothermal shaker at 303 K for 4 h.

Effect solutions contact time: A 25mL of 1000 mg/L of PNP were placed in several sample plastic bottles and shaken on the isothermal shaker for different time intervals (ranging from 5 min to 4 h) at 303 K, using adsorbent dose of 0.03g.

Effect of adsorbent dose: A 25mL solution of 1000 mg/L of PNP were placed in several sample bottles and shaken on the isothermal shaker to equilibrium at 303 K, using various mass of the activated carbon varying from 0.03 g to 0.2 g.

Effect of pH of the solution: A 25mL solutions of 1000 mg/L of PNP were placed in several sample bottles, the pH of the solution were varied using 0.1 M HCl and/or 0.1 M NaOH. The plastic bottles with the contents were shaken on the isothermal shaker till equilibrium was reached at 303 K, using an adsorbent dose of 0.03 g

Effect of temperature: Using the established equilibrium conditions of adsorptions, 25mL of the solutions were shaken at different temperature i.e. 303, 318 and 333 K.

Results and Discussion

Adsorbent characterization

Table 1 presents the comparison of physicochemical properties of PAC produced from PNS and that of a CGAC. The yield of pili active carbon obtained in this study is 38.4 % which fell within the percentage range yields of other nut shells (20.8 – 45.0 %) [13]. The pH of 3.8 obtained for PAC suggested that an L-type active carbon was produced while its conductivity value (391.5 µS/cm) indicated low ash content which could be attributed to washing of the PAC with deionised water severally. Its % bulk density value (0.51 g/cm^3) was found to be higher than minimum requirement (0.25 g/mL) for utilization as a commercial active carbon [14]. It was also higher than the reference commercial granular active carbon (BDH) value of 0.35 g/cm^3. The low ash contents of H_3PO_4 based active carbons are attributed to the leaching effect of the acid that increased with increase in concentration of the H_3PO_4 [15].

Figure 1 depicted the SEM micrographs at 1000 and 2500 magnifications and it revealed numerous pores with irregular shapes that indicated increase in contact area and easy pore diffusion during adsorption [16]. The XRD powder analysis of PAC and CGAC active carbons are presented in Fig. 2. There is a conspicuous peak at 2θ equal 24.0^o and 2θ equals 18^o for both the PAC and CGAC active carbons respectively and showed the crystalline nature of the active carbons.

The surface area, pore volume and pore size distribution are calculated from the initial plot of amount of N_2 gas adsorbed at STP against the relative pressures, P/P_o within the range of 0 – 1 for both PAC and CGAC active carbons (Fig. 3).

Table 1. **Physicochemical Properties of Active Carbons.**

Parameters	PAC	CGAC
Yield (%)	38.4±2.35	-
pH	3.80±0.14	3.12±0.12
Conductivity (µS/cm)	391.50±12.02	650±0.06
Moisture content (%)	18.55±0.35	17.5±0.33
Bulk Density (g/cm^3)	0.51±0.01	0.35±0.01
Pore Volume (cm^3/g)	0.422	0.208
Surface area (m^2/g)	960.1	426.3
Pore Size Distribution (nm)	2.842	3.300

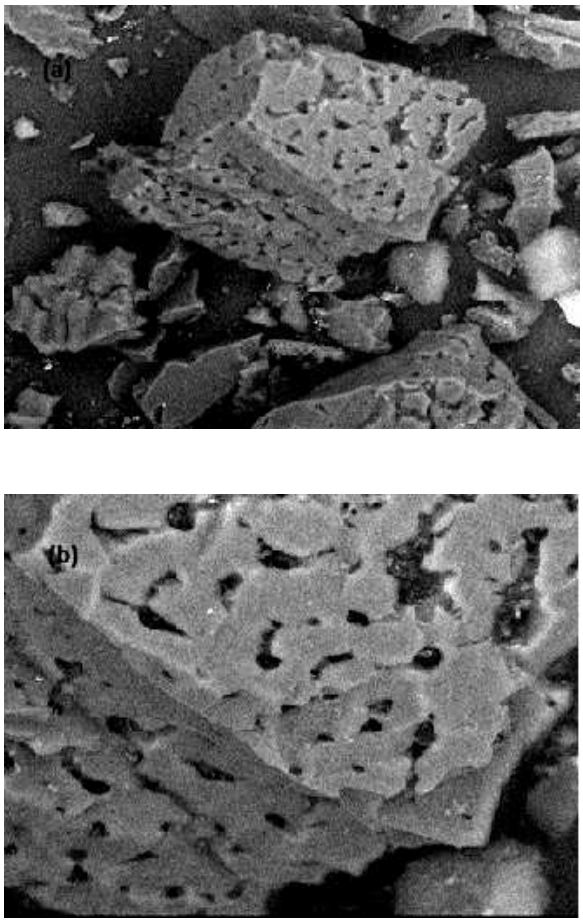

Figure 1. **SEM images of PAC. (a) x 1000; (b) x 2500**

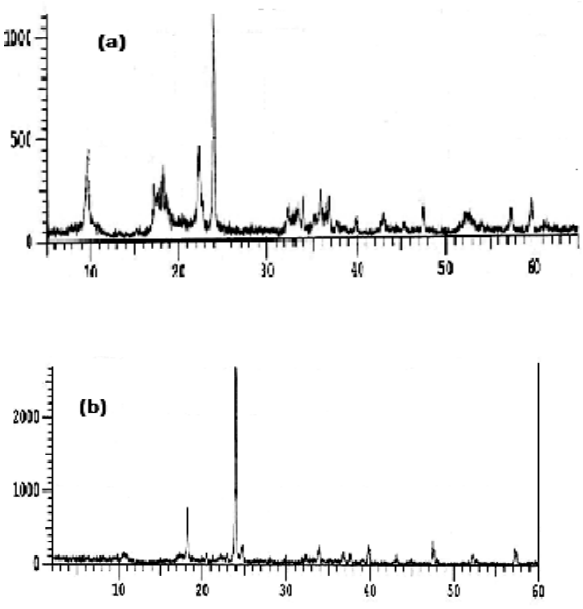

Figure 2. **XRD analysis of active carbons. (a) PAC; (b) CGAC**

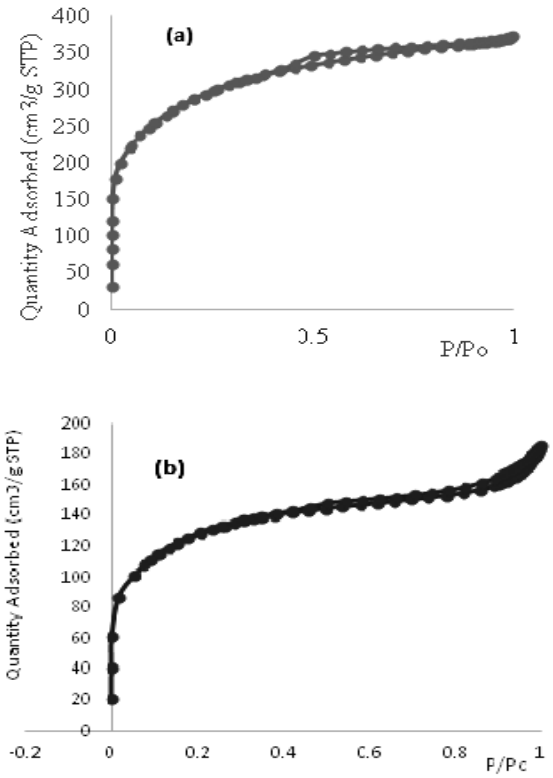

Figure 3. **The nitrogen adsorption isotherms of the active carbons. (a) PAC; (b) CGAC**

A surface area of 960.1 m^2/g and pore volume (0.422 cm^3/g) obtained for PAC are greater than surface area (426.3 m^2/g) and pore volume (0.208 cm^3/g) of commercial CGAC active carbons.

These values are within the minimum range of 500 – 1500 m^2/g needed for industrial application and removal of small molecules from aqueous solution [17]. The pore size distribution (2.84 nm) obtained for PAC could be classified as supper-microporous while that of CGAC (3.30 nm) as mesoporous. The physical observation of kneel in PAC is similar to that of CGAC which showed initial fast adsorption rate (Fig. 3). However, most average active carbon samples micropore volumes are generally between 0.2 – 0.5 cm^3/g with surface area of about 1000 m^2/g [18]. It has been reported that surface area in the range of 800 – 1300 m^2/g and total pore volume in the range of 0.3 - 0.8 cm^3/g of active carbon derived from olive stones are often used as precursors for high grade active carbon [19].

Influence of various factors on amount of PNP uptake

Effect of concentration: (Fig. 4a) shows the effect of the initial concentration (C_o mg/L) of PNP on the adsorption capacities of the prepared PAC and CGAC. As indicated in Fig. 4a, the amount adsorbed increased from 51.38 to 190.39 mg/g and 41.56 to 166. 97 mg/g as PNP concentration increased from 100 to 1000 mg/L and from 100 to 800 mg/L for PAC and CGAC respectively. This may be due to the fact that increasing the initial concentration of PNP would provide an important driving force to overcome all mass transfer resistances of PNP between adsorbate solution and the adsorbent surface [20]. Therefore the rate % which PNP molecules pass from the bulk solution to the particle surface will increase. Similar trends were observed in the adsorption of PNP on granular active carbon in basal salt medium in which amount adsorbed increased from 48.62 mg/g to 183.51 mg/g as the initial concentration of PNP increases from 10 mg/L to 1000 mg/L. Others with similar result in the adsorption of PNP using active carbon produced from different precursors are known [20.21, 22]. Further increase for both adsorbent brought a slight decrease in the amount of PNP adsorbed and thus concentrations of 1000 mg/L and 800 mg/L were chosen as equilibrium concentration for PAC and CGAC, respectively.

Effect of contact time: The effect of contact time of adsorbents is important in adsorption processes because it exercises a great deal of influence on the adsorption capacity of adsorbents. Fig 4b shows the variation in the quantity of PNP adsorbed by 0.03 g of PAC and CGAC at 303K with time. The rate at which adsorption occurred was rapid initially between 5 min to 30 mins, and became slower between 60 mins and 240 mins. This phenomenon may be due to a large number of available vacant surface sites for adsorption during the initial stage, and after a lapse of time, remaining vacant surface sites were difficult to be occupied due to repulsive force between solute molecules on the solid and bulk phases [21]. The high adsorption rate at the beginning of adsorption process by 0.03 g PAC and CGAC separately may also be due to the adsorption of PNP by exterior surface of the adsorbent. When saturation was reached at the exterior surface, the PNP molecules would then enter the pores of adsorbent and were adsorbed by the interior surface of the particles. This phenomenon takes relatively longer contact time (4 h) to reach equilibrium [22].

Different equilibrium times of 5 h, 60 min and 1 h has been reported for the adsorption of PNP with various adsorbent using NaOH modified palm oil fuel ash, amino-silane-activated palm oil fuel ash active carbon from coconut husk and commercial active carbon, respectively [20,23]. Another researcher obtained equilibrium after 5 h [24]. Thus, these differences in the time for adsorption process to reach equilibrium could be as a result of the functional groups present on the adsorbent as well as its surface morphology, such as the location and ease of access of the pores responsible for the adsorption.

Effect of adsorbent dose: (Fig. 4d) shows the adsorbent dose profile diagram for both adsorbents (PAC and CGAC). The amount of PNP adsorbed per gram of the active carbon decreased with increasing adsorbent dose. It decreased from 166.31 to 66.52 mg/L and from 138.30 to 50.55 mg/L for PAC and CGAC, respectively when adsorbent dose increased from 0.03 g to 0.20 g. Thus, for the remainder of the research, adsorbent dose of 0.03 g was used as the optimised adsorbent dose. This is similar to adsorbent dose reported during the adsorption of PNP using active carbon from coconut husk [23].

Effect of pH of the solution: Adsorption has been reported to be affected by the pH of the adsorbate [25]. As shown in (Fig. 4c), the adsorption of PNP on PAC and CGAC reduced from pH of 2 to 6 and remained relatively constant between pH 6 and 12. PNP exists as p-nitro phenolate anion when the solution pH > pKa and as neutral molecule when the solution pH < pKa [26]. Since the pKa of PNP is 7.12, PNP can be adsorbed on the adsorbent surface by electrostatic attraction when the PNP is ionized and by deprotonation or by a weak electrostatic attraction mechanism [27]. This occurs because PNP exists as a neutral molecule since is a weak polar compound [28]. Moreover,

PNP can also be adsorbed on the solid surface via a complex donor-acceptor mechanism [1]. In this study, the PNP was expected to have been adsorbed within the range of 2 to 6 via several other mechanism such as Van der Waals forces and complex donor-acceptor mechanism. However the PNP was more or less adsorbed at lower pH because it had been deprotonated and considering the fact that the pH of the adsorbents were 7.4 and 7.6 for PAC (after neutralising with NaOH) and CGAC respectively, then there exist an electrostatic repulsion between the adsorbent and the adsorbate at the higher pH range [20,29,30].

Effect of temperature: Plots of the amount adsorbed at equilibrium, q_e (mg/g) versus absolute temperature (K) are shown in (Fig. 4e) for both PAC and CGAC. It can be seen from these figures that the amount adsorbed decreases with increasing temperature for both adsorbents, indicating the apparent exothermic nature of the adsorption process. In the liquid phase, an increase in temperature commonly increases the solubility of the molecules and their diffusion within the pores of the adsorbent materials is hampered and hence at higher temperature adsorbed molecules tend to desorb suggesting physiosorption [23, 29, 30]. The effect of increase in temperature on adsorption capacity was more pronounced for the PAC than for the CGAC active carbons. At 303 K, the adsorption capacity of PAC decreased from 177.546 mg/g to 82.396 mg/g at 333 K and while at 303 K, CGAC decreased from 111.660 mg/g to 83.296 mg/g at 333K.

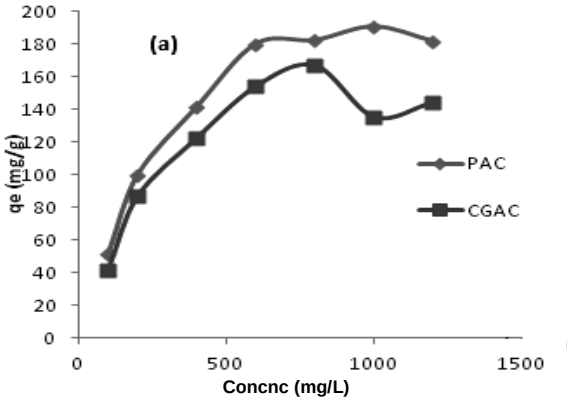

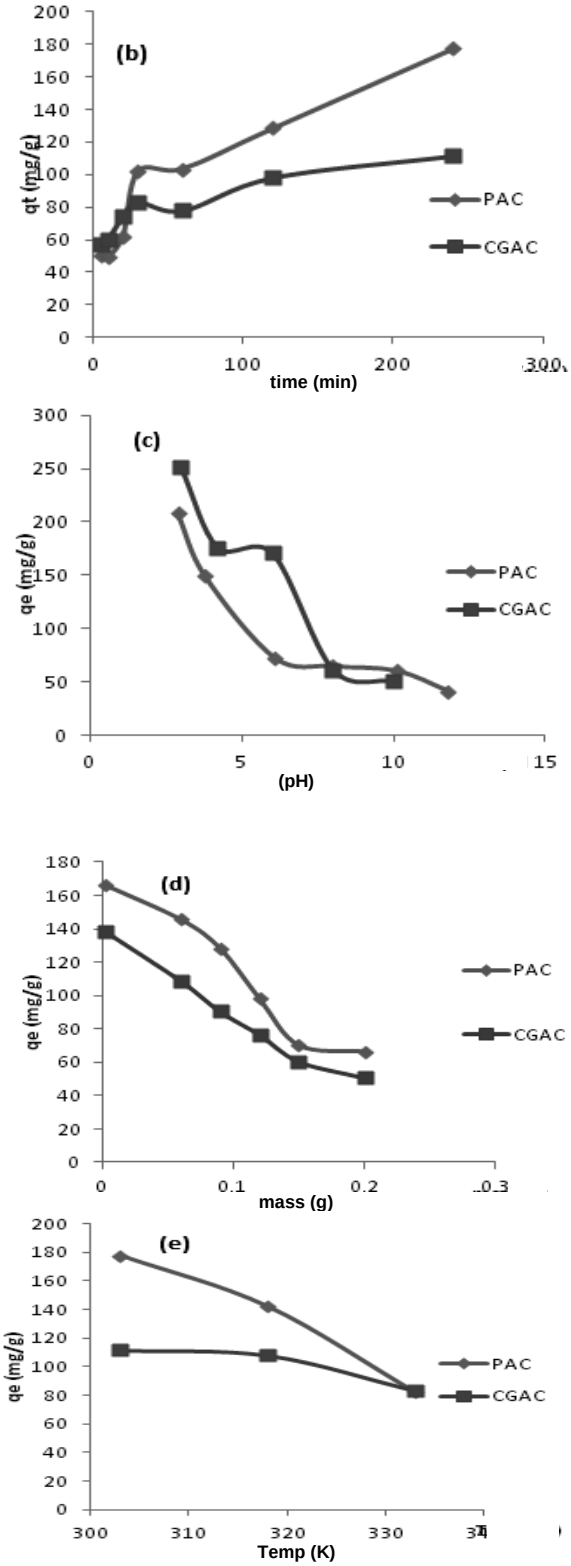

Figure 4. **Effect of adsorption conditions on adsorption capacities of the active carbons. (a) Initial Concentration; (b) Contact Time; (c) pH; (d) Adsorbent Dosage; (e) Temperature**

Equilibrium adsorption isotherms modeling

The equilibrium experimental data obtained were fitted into six adsorption isotherm models, namely; Langmuir, Freundlich, Temkin, Dubnin-Raduschkevich, Harkins-Jura and Halsey, and they all gave varying degree of success.

The langmuir adsorption isotherm model: This is based on the supposition of a homogeneous adsorbent surface with identical adsorption sites [31]. The linearized form of Langmuir equation is given as:

$$\frac{C_e}{q_e} = \frac{C_e}{q_{max}} + \frac{1}{b\,q_{max}} \qquad (2)$$

Table 2. **Adsorption Isotherm parameters.**

Isotherm		PAC	CGAC
Langmuir	q_{max} (mg/g)	250.0000	227.2727
	K_L	0.0063	0.0043
	R_L	0.1369	0.2238
	R^2	0.9968	0.9946
Freundlich	K_F (mg/g)	10.7770	4.9602
	1/n	0.4478	0.5593
	R^2	0.9499	0.9610
Temkin	B	49.6850	51.5450
	b_T	50.7022	48.8727
	A_T (L/mg)	0.0673	0.0409
	R^2	0.9835	0.9966
D-R	K_{od}	0.0024	0.0006
	q_D	169.9492	140.6958
	E (kJ/mol)	14.4334	28.8675
	R^2	0.8999	0.9180
Harkins-Jura	A_H	5000	2000
	B_H	3.5000	2.6000
	R^2	0.7550	0.7737
Halsey	n_H	-2.2334	-1.7879
	k_H	4.9465 x 10^{-3}	57.0845 x 10^{-3}
	R^2	0.9499	0.9610

PAC is active carbon produced at 723 K, 1:4, 2 h, CGAC is commercial granular active carbon; D –R means Dubunnin Radushkevih Adsorption Isotherm

The Langmuir plots of q_e/C_e versus C_e for both adsorbents are depicted in (Fig. 5a) and the Langmuir parameters obtained from the slope and intercept of the plots are listed in Table 2. Both exhibited high correlation coefficient, R^2 values of 0.9968 and 0.9946 for PAC and CGAC respectively.

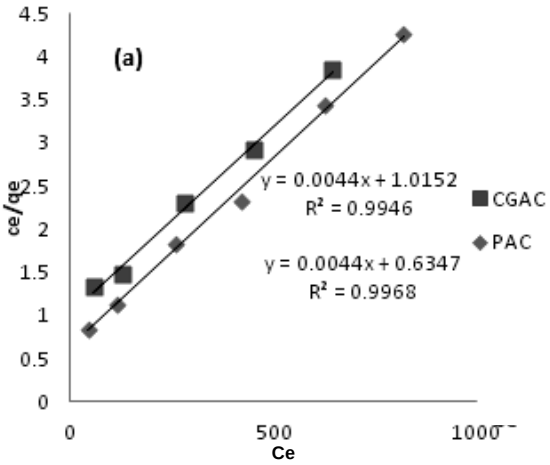

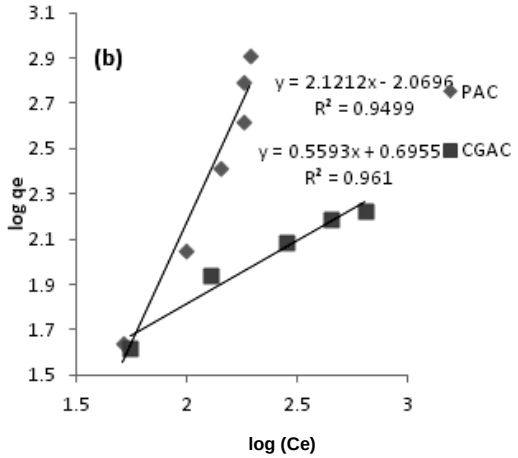

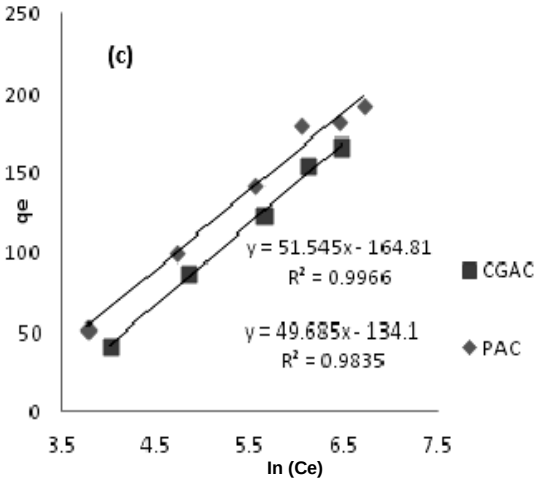

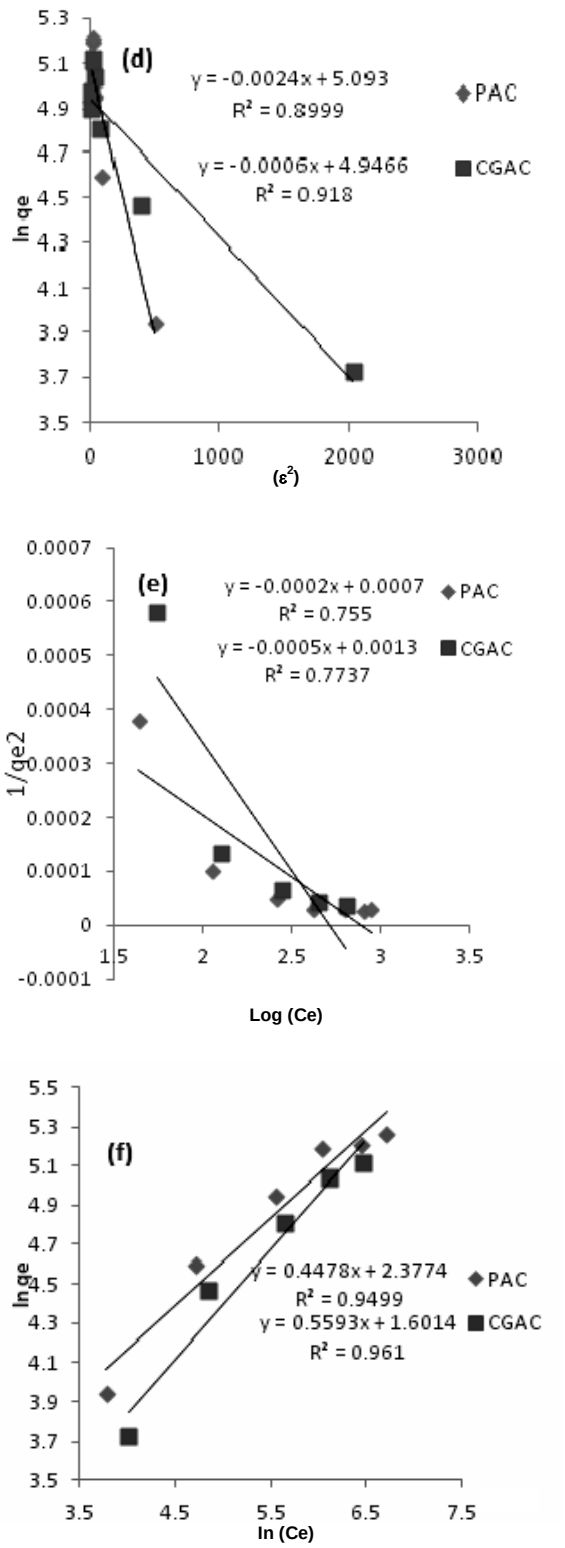

Figure 5. **Various adsorption isotherms for the removal of 4-NP using the active carbons. (a) Langmuir; (b) Freudlich; (c) Temkin; (d) Dubinin-Radushkevic; (e) Harkins Jura; (f) Halsey**

It can be observed from Table 2 that the PAC has an adsorption capacity (250 mg/g) higher than that of the CGAC (227.27 mg/g). Furthermore, a dimensionless separation factor, R_L equation is given in equation 3:

$$R_L = \frac{1}{1 + K_L C_e} \quad (3)$$

It expresses the essential characteristic of the Langmuir equation and indicates the nature of adsorption process, and its value was found to be in between 0 and 1 as listed in Table 2. This confirms that the adsorption of 4-nitrophenol is favourable on both active carbons. Similar results have been obtained by several authors for the adsorption of PNP and phenol using various adsorbents [23, 31, 32].

Freundlich adsorption isotherm model: suggests neither homogeneous site energies nor limited levels of adsorption which implies that it can describe the experimental data of adsorption isotherm whether adsorption occurs on homogeneous or heterogeneous sites and it is not controlled by the formation of the monolayer [33]. The linearized Freundlich equation is given as:

$$\log \frac{x}{m} = \log K + \frac{1}{n} \log C_e \quad (4)$$

From the slope and intercept of the linear plots of ln q_e versus ln C_e; (Fig. 5b), Freundlich parameters 1/n and K_F indicating the measures of adsorption capacity of PAC and its intensity of adsorption respectively, were obtained and listed with the correlation coefficient value, R^2 (Table 2).

The results revealed that the adsorption of phenol on PAC and CGAC obeys both Freundlich and Langmuir adsorption isotherms, as indicated by high R^2 Values (> 95%). Moreover, the Freundlich constant (K_F = 10.777 mg/g) of PAC is also larger than that obtained for CGAC (K_F = 4.960 mg/g). The results indicated that PAC has higher adsorption affinity towards 4-nitrophenol than CGAC [25]. This might be due to larger surface area of PAC as a result of its highly porous nature, which makes PAC more effective in the adsorption process. The value of 1/n indicates a favourable adsorption when $0 < 1/n < 1$ [33]. The adsorption intensity, 1/n is found to be 0.448 and 0.559 for PAC and CGAC, respectively. It is

observed that both adsorbents satisfy the conditions of heterogeneity.

Temkin adsorption isotherm: assumes that the heat of adsorption of all the molecules in the layer is inversely proportional to coverage of the adsorbent surface which might be attributed to adsorbate species – adsorbent interactions. A uniform distribution of binding energies up to some maximum binding energy is the characteristics of Temkin adsorption [34]. The linear form of the Temkin isotherm is represented in equation (5):

$$q_e = \frac{RT}{b_T} \ln A_T + \left(\frac{RT}{b_T}\right) \ln C_e \quad (5)$$

and

$$B = \frac{RT}{b_T} \quad (6)$$

Figure 5(c) depicts the Temkin isotherm plots for the PNP uptake onto the active carbons from which the relevant Temkin adsorption isotherm values are obtained and are shown with values of correlation coefficients in Table 2. The B values indicates the heat of adsorption obtained as 49.685 and 51.545 for PAC and CGAC respectively, while A_T representing the equilibrium binding energy are 0.0673 (L/mg) and 0.0409 (L/mg) for PAC and CGAC, respectively. Thus, these values imply that the PNP are more strongly adsorbed on the PAC surface than that of CGAC indicating that there is a stronger interaction between PNP and the respective active carbon. Similar results have been reported as per the adsorption of methyl orange using pinecone derived active carbon [35]. They reported B_T value of 24.292 and A_T value of 0.162.

Dubinin-Radushkevich isotherm: The linear expression of Dubinin-Radushkevich isotherm is:

$$\ln q_e = \ln q_s - K_{ad}\, \varepsilon^2 \quad (7)$$

$$E = \left[\frac{1}{\sqrt{2K_{ad}}}\right] \quad (8)$$

$$\varepsilon = RT \ln\left(1 + \frac{1}{C_e}\right) \quad (9)$$

Radushkevich and Dubinin showed that there is a relationship between porous structure of sorbent and characteristic sorption curve obtained from adsorption data. As solute molecules of PNP move to adsorbent surface from bulk of the solution, a relationship between the mean free energy; E of sorption per mole of the sorbate and the constant, K_{ad}, is established. The energy, E and the parameter ε can be derived using equations 8 and 9 respectively. Equation 7 represents the linear expression of the Dubinin–Radushkevich isotherm and the plot of ln q_e versus ε^2 is depicted in Fig. 5(d).

Table 2 reveals k_{ad}, $q_{m,}$ E, and R^2 values. The adsorption capacities, q_m values of 169.949 mg/g and 140.696 mg/g were obtained for PAC and CGAC, respectively. These values are less than 250.0 mg/g and 227.272 mg/g as Langmuir adsorption capacity for PAC and CGAC respectively. This might be as a result of variations in experimental conditions. The q_m values of 25.94 mg/g and 26.06 mg/g calculated from Dubinin-Radushkevich isotherm for the uptake of congo red using leaves of water melon rinds and neem-tree have been reported [36]. These lower values might be as a result of the fact that adsorbents employed are biosorbents and not active carbon.

Generally, the accepted adsorption energy value range of 1.00 - 8.00 and 8.00 - 16.00 kJ/mol indicated physical and chemical adsorption, respectively [30]. The E values of 14.433 kJ/mol for PAC and 28.868 kJ/mol CGAC indicated chemical adsorption for both adsorption systems. However, E values of (0.29 – 0.32 kJ/mol) and < 8 kJ/mol have been obtained by other researchers that indicated physiosorption [36.37] in the removal of direct red dye.

Harkins-Jura adsorption isotherm model

The existence of heterogeneous pore distribution explains the occurrence of multilayer adsorption. The model can be expressed as [35]:

This can be linearised to give the following equation

$$\frac{1}{q_e^{\,2}} = \left(\frac{B_H}{A_H}\right) - \left(\frac{1}{A_H}\right)\log C_e \qquad (10)$$

Where A_H and B_H are isotherm parameter and constant.

The plot of $1/q_e^2$ versus log C_e is presented in Fig. 5(e) and values of Harkin-Jura constants and R^2 for both active carbons are shown in Table 2. The R^2 values of Harkins Jura plots obtained are 0.7550 and 0.7737 for PAC and CGAC, respectively which are lower than values of Langmuir isotherm whose R^2 values within range of 0.9499 – 0.9610 for PAC and CGAC. Thus, it can be assumed that the adsorption process might not be multilayer.

Halsey adsorption isotherm: is one of adsorption isotherms that explains multilayer adsorption and is represented in Eqn. 11 [38]. Hetero porous nature of adsorbent is normally implied if experimental adsorption data fits into Halsey adsorption isotherm equation.

$$q_e = e^{\frac{\ln k_H - \ln C_e}{n}} \qquad (11)$$

The above equation can be linearized to obtain:

$$\ln q_e = \left[\left(\frac{1}{n_H}\right)\ln k_H\right] - \frac{1}{n_H}\ln C_e \qquad (12)$$

Where k_H and n_H are empirical isotherm constant and exponents, respectively. From the plot of ln q_e vs. ln C_e (Fig. 5f), values of Halsey constants, k_H and n_H as well as their R^2 for PAC/PNP and CGAC/PNP adsorption systems are depicted in Table 2. The n_H values obtained (-2.2334 and -1.7879) for PAC and CGAC respectively are similar to -2.224 and dissimilar to 1.82 and 1.78 obtained by other researchers [35,37]. If adsorption increased with decrease in n_H values, then it indicates adsorption process to be endothermic [37] which might be attributed to the differences in adsorbent-adsorbate system.

The parameters obtained for the various adsorption isotherms equations of both the PAC-PNP and CGAC-PNP adsorption system are presented in Table 2. The correlation Coefficient factor, R^2 obtained indicated experimental data obtained in this study fitted well into the various adsorption isotherms investigated. On basis of correlation coefficient, R^2, the six investigated isotherm models could be arranged in decreasing order of favoured adsorption isotherm as follows: Langmuir > Temkin > Freundlich = Halsey > Dubinin-Radushkevich > Harkin-Jura for both PAC and CGAC active carbons with exception of Temkin that comes before Langmuir for CGAC. Langmuir and Temkin isotherms exhibited highest correlation coefficients, R^2 among other isotherms and depict homogeneity of the surface of PAC and CGAC as well as the monolayer adsorption nature of PNP onto the adsorbents. Therefore, Langmuir and Temkin isotherm showed to best fit the equilibrium data for adsorption of PNP on PAC and CGAC.

Adsorption kinetics studies: The kinetic experimental data obtained for the adsorption of PNP on PAC and CGAC were interpreted by means of pseudo-first order, pseudo-second order, intra-particle diffusion and Elovich kinetic models.

Pseudo-first order and pseudo-second order kinetic models

The linear forms of pseudo-first order and pseudo-second order kinetic model equations are given in Eqns. 13 and 14. Despite, these models do not fit well for the whole range of contact times, the initial 20 to 30 min of adsorption process were applicable [31].

$$\log(q_e - q_t) = \log q_e - \frac{k_1 t}{2.303} \qquad (13)$$

$$\frac{t}{q} = \frac{1}{k_2 q_e^{\,2}} + \frac{1}{q_e} \qquad (14)$$

The plot of linearized form of the equation is shown in Fig. 6(a). The pseudo first-order rate constant K_1, amount of PNP adsorbed at equilibrium q_e and correlation coefficients are shown in Table 3. The results showed that the correlation coefficients, R^2 obtained for both adsorbents for pseudo first order kinetics model (0.8761 and 0.876) were lower than their corresponding pseudo second order kinetics model (R^2 = 0.9626, 0.9906) and the experimental q_e

(177. 56 and 111.66 mg/g) did not agree with the calculated q_e (125.81 and 52.30 mg/g) obtained from the linear plots of PAC and CGAC, respectively. Therefore, adsorption of PNP onto the active carbons revealed that pseudo-first-order kinetic model failed to explain the kinetic adsorption process.

Although the pseudo-first order equation provides a fairly good fitting (R^2 = 0.8761 and 0.8776) to the experimental data point, the pseudo-second order kinetic model (R^2 = 0.9626, 0.9906) describes the kinetic data better. This may be due to the fact the adsorption rate of PNP onto both active carbons depends on the behaviour over a whole range of adsorption process rather than depending on the initial 20 to 30 min as pseudo-first order kinetic model, as similarly reported by others [3]. (Fig. 6b) shows the plots of t/q against t and the resulting kinetic parameters are presented in Table 3. The calculated values of q_e of 192.307 mg/g and 114.942 mg/g were closer to the experimental q_e values of 177.56 mg/g and 111.66 mg/g for PAC and CGAC, respectively.

However, an inconsistency in the agreement of the experimental q_e and calculated q_e for the adsorption of PNP with granular active carbon has been reported [24]. Experimental q_e value of 27.41 mg/g was reported and values of 95.70 mg/g and 99.74 mg/g were reported for pseudo-first and pseudo-second kinetic models respectively. Moreover, it has been reported that pseudo-first order rates of 0.0104 /min and pseudo-second order rate of 0.0003 g/mg/min which are similar to values obtained in this study, with rate constants of 0.0083 /min and 0.0111 /min for pseudo-first kinetic models and pseudo-second order rates of 0.00015 g/mg/min and 0.00066 g/mg/min for PAC and CGAC, respectively [39].

The movement of solute molecules on to solid surface particulates from the aqueous phase, and then diffusion of the solute molecules into the pore interiors [37] could be described by the intra-particle diffusion rate equation and is given as [32]:

$$q_t = k_{id} t^{1/2} + C \quad (15)$$

where k_{id} and C are the intra-particle diffusion rate constant and boundary layer thickness, respectively. The plotting q_t against $t^{1/2}$ as shown in (Fig. 6c) indicates the effect of pore diffusion. The general features of an initial steep linear portion and plateau are attributed to the bulk diffusion; intra-particle diffusion and the plateau portion represent the equilibrium. The magnitudes of k_{id}, C and the corresponding regression coefficients of both the adsorption system are listed in Table 3. The pore diffusion rate constant, k_{id}, values; 9.668 mg/g $min^{1/2}$ and 3.9902 mg/g $min^{1/2}$ indicated substantial diffusion of PNP onto PAC and CGAC active carbons.

The existence of linear relationship between amount qe against $t^{1/2}$ indicates that intra-particle diffusion participated during the adsorption process. If the straight line of the plot of qe against $t^{1/2}$ passes through the origin, then intra particle diffusion becomes the controlling step. However, if the straight line does not pass through the origin, it indicates that the intra particle diffusion is not the only controlling step but that boundary surface effects are also involved [20].

The pore diffusion rate constant of 0.46 mg/g $min^{1/2}$ and 0.161 mg/g $min^{1/2}$ in the adsorption of PNP with Zeolite and Bentonite have been obtained [31]. The difference in this value and those obtained in this study shows that the prepared PAC contains more pores available for adsorption than the natural Zeolite and Bentonite. This is similar to the adsorption of direct red dye 81 with bamboo sawdust and treated bamboo sawdust where k_{id} values of 0.32 mg/g $min^{1/2}$ and 0.62 mg/g $min^{1/2}$ were obtained.

Moreover, k_{id} value of 3.2479 mg/g $min^{1/2}$ has been obtained in the adsorption of phenol using active carbon from olive stones [32]. The adsorption of PNP using active carbon fibre and granular active carbon gave similar result obtained in this study with k_{id} values of 8.924 mg/g $min^{1/2}$ and 11.91 mg/g $min^{1/2}$, respectively [23].

The adsorption data could also be treated using Elovich equation that is shown in equation 16 [31]:

$$\frac{dq_t}{dt} = \alpha e^{\beta q_t} \quad (16)$$

This on linearising and simplifying can be written as:

$$q_t = \frac{1}{\beta}\ln(\alpha\beta) + \frac{1}{\beta}\ln(t) \quad (17)$$

where α (mg/g min) and β (g/mg) are the initial adsorption rate constant and desorption rate constant, respectively. Kinetics of adsorption of PNP with PAC and CGAC also followed Elovich equation with the plots of q_t against ln t giving straight lines with fairly high correlation coefficient (Fig. 6d). The Elovich constants α, β computed from the plots are 18.248 mg/g min, 0.0305 g/mg for PAC and 133.823 mg/g min, 0.0721 g/mg for CGAC as given in Table 3. These values might also explain why the adsorption process took longer time to reach equilibrium.

It has been reported that α, β values of 1.10 mg/g min and 1.05 g/mg were obtained for the removal of methyl orange using bamboo sawdust and 2.23 mg/g min and 0.58 g/mg when using acid treated Bamboo Sawdust indicating that the treatment increased the ability of the adsorbent to adsorb more and reach equilibrium faster than the raw sample [37].

The comparison of correlation coefficients obtained for pseudo-second order kinetic model (R^2 = 0.9626, 0.9906) explained the adsorption process better than Elovich model (R^2 = 0.9063 and 0.9286). However, in overall, the pseudo-second order kinetic model still appears to be the rate determining model as it is the model with the highest correlation coefficient values (Table 3).

Table 3. **Kinetic Parameters of Adsorption of PNP.**

Kinetic Model		PAC	CGAC
Pseudo 1st	k_1 (min^{-1})	8.2908 x 10^{-3}	11.1054 x 10^{-3}
	q_e (mg/g)	125.8056	52.2998
	R^2	0.8761	0.8776
Pseudo 2nd	k_2 ($gmg^{-1}min^{-1}$)	1.5131 x 10^{-4}	6.6570 x 10^{-4}
	q_e (mg/g)	192.3077	114.942
	R^2	0.9626	0.9906
Intra-particle diffusion	k_{id} ($mg/gmin^{1/2}$)	9.668	3.9902
	C	27.744	52.043
	R^2	0.9508	0.9232
Elovich	α	18.248	133.823
	β	0.0305	0.0721
	R^2	0.9063	0.9286

PAC means Pilli nut active carbon; CGAC indicates commercial granular activated carbon

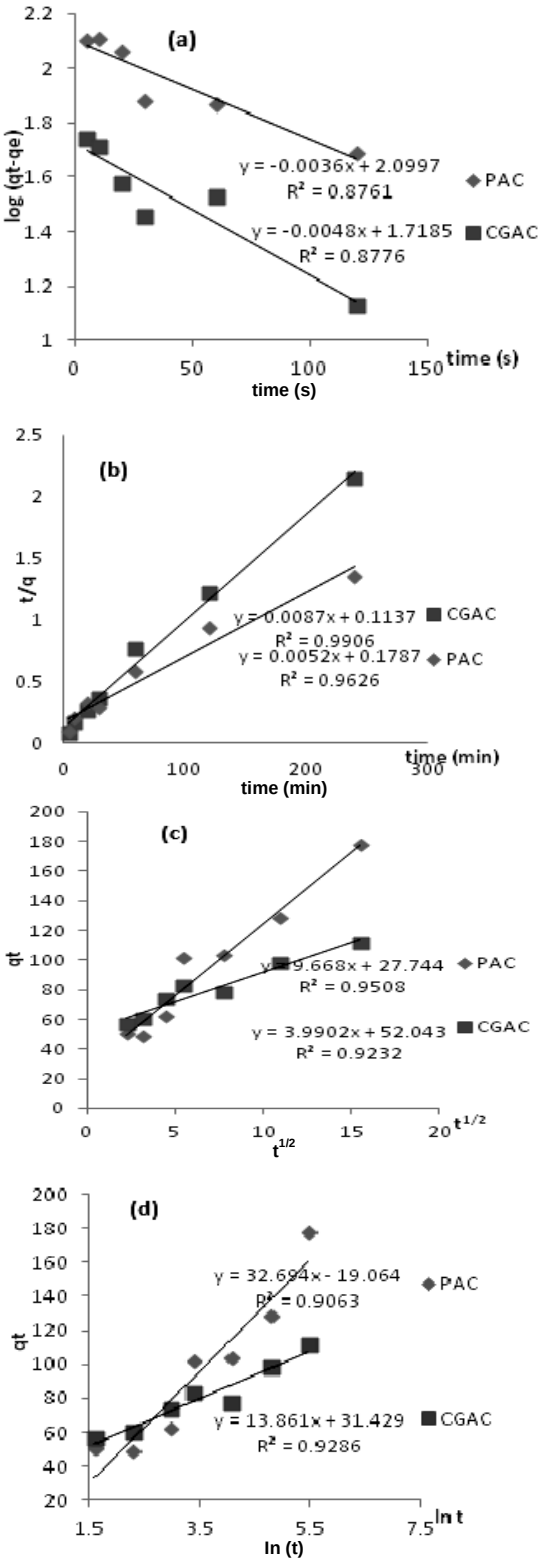

Figure 6. **Kinetic Models fit of adsorption of 4-NP with the active carbons. (a) Pseudo-First; (b) Pseudo-Second; (c) Intra-particle; (d) Elovich**

Thermodynamics studies: Thermodynamic parameters can provide useful and strong information about the mechanism involved in the adsorption process. The characterization of equilibrium system like the adsorption system in this study are described by thermodynamic parameters such as free energy (ΔG), enthalpy (ΔH) and entropy (ΔS) changes which were calculated using Eqns. 18 to 21.

$$\ln k_2 = \ln A - \frac{E_a}{RT} \quad (18)$$

$$\ln K = -\frac{\Delta H}{RT} + \frac{\Delta S}{R} \quad (19)$$

$$\Delta G = -RT \ln K \quad (20)$$

$$K = \frac{C_i - C_f}{C_i} \quad (21)$$

Where k_2 is the pseudo second order rate constant, A is pre-exponential factor of the Arrhenius equation, E_a is the activation energy of the reaction, R is gas constant (8.314 $Jmol^{-1}K^{-1}$), T is absolute temperature in K, C_i is initial concentration before adsorption and C_f is concentration left in solution after adsorption. The thermodynamic plots obtained from Eqns. 19 to 21 are depicted in Fig.7a while the values of ΔG, ΔH, ΔS and E_a for both adsorbents are listed in Table 4.

As seen from Table 4, the negative values of the enthalpy, entropy and free energy changes indicate exothermic nature of the processes, decrease in disorderliness and that the adsorption processes is spontaneous and feasible.

Moreover the ΔH values of adsorption of PNP with PAC (-17.338 kJ/mol) as well as CGAC (-8.430 kJ/mol) lie between 2.1 and 20.9 kJ/mol indicating that adsorption of PNP can be classified as physiosorption [40] for both PAC and CGAC. Furthermore, PAC shows higher adsorption enthalpy changes than the CGAC, which signifies that PAC has a stronger affinity for PNP than CGAC [41].

The thermodynamic results obtained in this study are in agreement with the results observed by other researchers [23, 29, 30, 41]. The ΔH values of -29.46 kJ/mol and -17.76 kJ/mol obtained for active carbon fiber and granular active carbon in the adsorption of PNP as well as ΔH values of -4.4347 kJ/mol and -7.766 kJ/mol in the adsorption of PNP using natural Zeolite and Natural Bentonite have been reported [23, 31].

Table 4. **Thermodynamics Parameters.**

Adsorbent / Temp (K)	E_a (kJ/mol)	ΔH (kJ/mol)	ΔS (J/mol)	ΔG (kJ/mol) *303*	*318*	*333*
PAC	39.887	-17.338	-69.162	-3.700	-4.473	-5.792
CGAC	-	-8.430	-41.990	-4.384	-4.692	-5.665

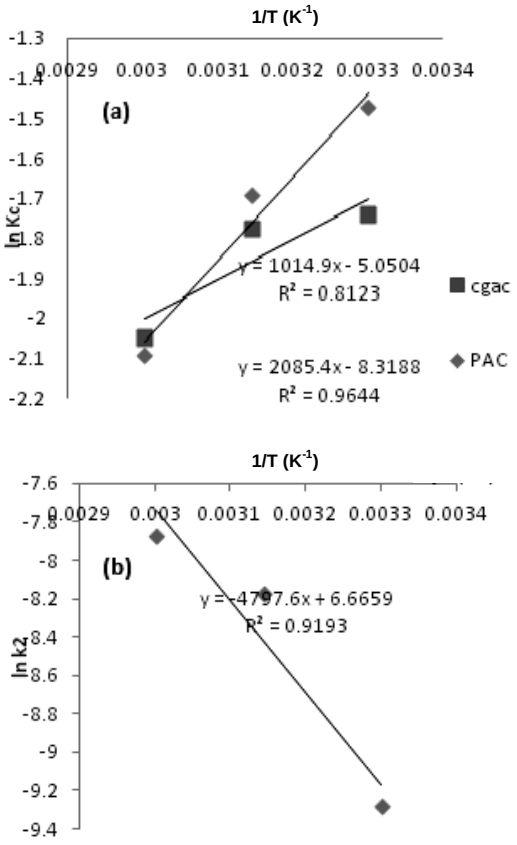

Conclusion

PAC prepared from PNS adsorbed PNP better than CGAC. The BET specific surface area and total pore volume of PAC were higher than those of CGAC while pore size distribution of PAC classified it as super-micro porous. The amounts of PNP adsorbed by both adsorbents were

strongly influenced by experimental conditions. Langmuir isotherm best described the adsorption of PNP on the PAC while pseudo-second-order kinetic model fitted well with the experimental data of both activated carbons. Intra particle diffusion alone could not describe the rate determining mechanism for the adsorption processes. The adsorption process was found to be exothermic and spontaneous. Thus, there is high potential ability of PAC to remove PNP from aqueous solution and could also be utilize for removal of gas and small size molecules from industrial effluents.

Reference

1. K. Arinjay, K. Shashi, K. Surendra, V. Dharam and B. Gupta, *J. Hazard. Mater*., 147 (2007) 155. https://doi.org/10.1016/j.jhazmat.2006.12.062
2. J. Michalowicz and W. Duda, *Polish J. Environ. Stud*., 16 (2007) 347.
3. ATSDR (Agency for Toxic Substances and Disease Registry). *US Department of Health and Human Services, USA*. (1998).
4. BIS Tolerance Limit for Industrial Effluents Discharged into Inland Surface Waters: Coke Oven *IS 2490 (Part 1), Bureau of Indian Standards, New Delhi. (*1974).
5. A. A. Hatem, M. M. Jamil, Y. Rosiyah, B. Radzi and M. Abas, *Asian J. Chem.*, 25 (2013) 9573.
6. M. C Burleigh, M. A. Markowitz, M. S. Spector and B. P. Gaber, *Environ. Sci. Technol.*, 36 (2002) 2515. https://doi.org/10.1021/es011115l
7. K. Srinivasan, P. B. S. Rao and A. Ramadevi, *Ind. J. Environ. Hlth*, 30 (1998) 303.
8. V. P. Vinod and T. S. Anirudhan, *J. Sci. Ind. Res.*, 61 (2002) 128.
9. M. M. Gómez-Tamayo, A. Marcías-García, M. A. Díaz-Díez and E. M. Cuerda-Correa, *J. Harzard. Mater.*, 153 (2008) 28.
10. American Society for Testing and Materials Annual Book of ASTM Standard. ASTM, Philadelphia PA (1996) 15.01
11. C. A. Toles, W. E. Marshall and M. M. Johns, *Carbon*, 37 (1999) 1207. https://doi.org/10.1016/S0008-6223(98)00315-7
12. M. Ahmedna, W.E. Marshall and R. M. Rao, *Bioresour. Technol.*, 71 (2000) 113. https://doi.org/10.1016/S0960-8524(99)00070-X
13. L. H. Wartelle and W. E. Marshall, *J. Chem. Technol. Biotechnol.*, 76 (2001) 451. https://doi.org/10.1002/jctb.408
14. American Water Works Association (AWWA) standard for granular activated carbon. *American Water Works Association, ANSI / AWWA B604 – 90*, Denver Co. (1991).
15. B. Corcho-Corral, M. Olivares-Marín, C. Fernández-González, V. Gómez-Serrano and A. Macías-García, *Appl. Surf. Sci.*, 252 (2006) 5961. https://doi.org/10.1016/j.apsusc.2005.11.007
16. J. B. Patel and P. Sudhakar, *Electr. J. Environ. Agric. Food Chem.*, 7 (2008) 2735.
17. R. C. Bansal, M. Goyal, *Activated Carbon Adsorption.* Taylor and Francis Group, published by CRC press UK. (2005) 497.
18. H. Jankowska, A. Swiatkowski, J. Choma, *Active Carbon*, Ellis-Harwood, Chichester, UK, (1991) 50.
19. A. Linares-Solano, G. Rodriguez-Reinoso, M. Molina-Sabio and J. D. Lopez-Gonzalez, *Adv. Sci. Technol.*, 1 (1984) 223.
20. A. A. Hatem, M. M. Jamil, A. A. Ahmad and M. Radzi Bin Abas, *J. Purity Utility Reaction Environ.*, 1 (2012a) 104.
21. A. A. Ahmed, B. H. Hameed and N. Aziz, *J. Hazard. Mater.*, 141 (2007) 70. https://doi.org/10.1016/j.jhazmat.2006.06.094
22. M. Sathishkumar, A. R. Binupriyu, D. Kavitha and S. E. Yun, *Biores. Technol.*, 98 (2007) 866. https://doi.org/10.1016/j.biortech.2006.03.002
23. A. A. Hatem, M. M. Jamil, Y. Rosiyah and M. Bin Radzi Abas, *Asian J. Chem.*, 25 (2013) 9573.
24. S. Suresh, V. C. Srivastava and I. M. Mishra, *Chem. Ind. Chem. Eng. Quarterly*, 19 (2013) 195. https://doi.org/10.2298/CICEQ111225054S

25. S. Rengaraj, M. Seuny-Hyeon and R. Sivabalan, *Waste Manag.*, 22 (2002) 543. https://doi.org/10.1016/S0956-053X(01)00016-2
26. J. M. Li, X. G. Meng, C. W. Hu and J. Du, *Biores. Technol.*, 100 (2009) 1168. https://doi.org/10.1016/j.biortech.2008.09.015
27. B. B. Tewari and M. Boodhoo, *J. Coll. Inter. Sci.*, 289 (2005) 328. https://doi.org/10.1016/j.jcis.2005.04.032
28. N. Calace, E. Nardi, B. M. Petronio and M. Pietroletti, Environ. *Pollut.*, 118 (2002) 315. https://doi.org/10.1016/S0269-7491(01)00303-7
29. D. Tang, Z. Zheng, K. Lin, J. Luan and J. Zhang, *J. Hazard. Mater.*, 143 (2007) 49. https://doi.org/10.1016/j.jhazmat.2006.08.066
30. L. M. Cotoruelo, M. D. Marques, F. J. Diaz, J. Rodriguez–Mirasol, J. J. Rodriguez and T. Cordero, *Chem. Eng. J.*, 184 (2012) 176. https://doi.org/10.1016/j.cej.2012.01.026
31. G. .Varank, A. Demir, K. Yetimezsoy, S. Top, E. Sekman and M. S. Bilgili, *Indian J. Chem. Technol.*, 19 (2012) 7.
32. T. Bohli, N. Fiol, I. Villaescusa and A. Ouederni, *J. Chem. Eng. Process. Technol.*, 4 (2013) 165. https://doi.org/10.4172/2157-7048.1000158
33. N. A. Halif, W. M. A. W. Daud, I. M. Noor, and C. R. C. Hassan, *AEESEAP J.*, 31 (2007) 23.
34. M. I. Tempkin and V. Pyzhev, *Acta Phys. Chim. USSR*, 12 (1940) 327.
35. M. R. Samarghandi, M. Hadi, S. Moayedi and A. F. Barjasteh, *Iran J. Environ. Health Sci. Eng.*, 6 (2009) 285.
36. M. B. Ibrahim and S. Sani, *Open J. Phy. Chem.*, 4 (2014) 139.
37. T. A. Khan, S. Dahiya and I. Ali, *Gazi University J. Sci.*, 25 (2012) 59.
38. C. A. Basar, *J. Hazard. Mater.*, 135 (2006) 232. https://doi.org/10.1016/j.jhazmat.2005.11.055
39. B. H. Hameed, *Colloid. Surf.A: Physicochem. Eng.*, 307 (2007) 45. https://doi.org/10.1016/j.colsurfa.2007.05.002
40. S. K. Theydan and M. J. Ahmed, *J. Anal. Appl. Pyrol.*, 97 (2012) 116. https://doi.org/10.1016/j.jaap.2012.05.008
41. A. Li, H. Wu, Q. Zhang, G. Zhang, C. Long, Z. Fei and F. Liu, *Chinese J. Polymer Sci.*, 22 (2004) 259.